Rare Met. (2020) 39(6):688–694
https://doi.org/10.1007/s12598-018-1124-9

RARE METALS
www.editorialmanager.com/rmet

Ti–Zr–Cu–Fe–Sn–Si–Ag–Ta bulk metallic glasses with good corrosion resistance as potential biomaterials

Ying Liu, Hao-Jie Wang, Shu-Jie Pang*, Tao Zhang

Received: 13 June 2018 / Revised: 25 June 2018 / Accepted: 19 July 2018 / Published online: 12 September 2018

Abstract $Ti_{47}Cu_{38-x}Zr_{7.5}Fe_{2.5}Sn_2Si_1Ag_2Ta_x$ (x = 1–4; at%, the same below) bulk metallic glasses (BMGs) with good bio-corrosion resistance and mechanical properties were fabricated by copper mold casting. Critical diameter of the Ti-based BMGs with 1 at%–4 at% Ta was 3 mm. The Ta-incorporated Ti-based BMGs exhibit higher open current potential and parallel passive current density in comparison with those of Ti–6Al–4V alloy in 0.9 wt% NaCl and Hank's solution, implying their good corrosion resistance. The pitting corrosion potential of the Ti-based BMGs gradually increases up to about 1.25 V with Ta addition increasing up to 4 at% in 0.9 wt% NaCl solution. Among the present Ti-based BMGs, the alloy bearing 2 at% Ta exhibits the optimal integration of mechanical properties, including the compressive fracture strength exceeding 2000 MPa, relative low Young's modulus of 98 GPa, plastic strain of 3.4% and high hardness of HV 599. The Ta-bearing Ti-based bulk metallic glasses with integration of relative high GFA, good mechanical properties and high bio-corrosion resistance are beneficial for biomedical applications.

Y. Liu, H.-J. Wang, S.-J. Pang*, T. Zhang
Key Laboratory of Aerospace Materials and Performance (Ministry of Education), School of Materials Science and Engineering, Beihang University, Beijing 100191, China
e-mail: pangshujie@buaa.edu.cn

Y. Liu
School of Physics and Nuclear Energy Engineering, Beihang University, Beijing 100191, China

S.-J. Pang
Beijing Advanced Innovation Centre for Biomedical Engineering, Beihang University, Beijing 100191, China

Keywords Ti-based alloy; Bulk metallic glass; Glass forming ability; Bio-corrosion resistance; Mechanical properties

1 Introduction

Ti-based bulk metallic glasses (BMGs) with good mechanical properties, superior bio-corrosion resistance, good biocompatibility as well as good formability have attracted great attentions to be used as potential biomaterials [1–10]. Great efforts have been devoted to designing and synthesizing biomedical Ti-based BMGs free from highly toxic elements with high glass forming ability (GFA) [2–5]. Recently, Ni-free Ti–Cu–Zr–Fe–Sn–Si(–Ag, Sc) BMG systems as potential biomaterials have been developed based on the three empirical rules, confusion rule and the coexistence of similar and different elements rule for designing glassy alloy compositions [3–5, 11–14]. In particular, the $Ti_{47}Cu_{38}Zr_{7.5}$ $Fe_{2.5}Sn_2Si_1Ag_2$ BMG with critical diameter of 7 mm is the largest Ni- and Be-free Ti-based BMG-bearing low content of noble element [4]. The $Ti_{45}Cu_{40}Zr_{7.5}Fe_{2.5}Sn_2Si_1Sc_2$ BMG with critical diameter of 6 mm exhibited large compressive plastic strain up to about 6% [5]. Integration of good mechanical properties, bio-corrosion resistance and in vitro biocompatibility of these Ti-based BMGs indicated their potential as biomaterials. Potentiodynamic polarization of these Ti-based BMGs revealed that pitting corrosion occurred at relatively high potential. Generally, pitting corrosion is apt to aggravate the release of metallic ions which could cause adverse biological responses and lead to gradual deterioration of mechanical properties [15, 16]. The aggressive physiological environment in human body, which

comprises amino acids, organic acids, proteins and many inorganic ions such as chlorine, could induce corrosion of metallic biomaterials once they are implanted [17, 18]. High bio-corrosion resistance is necessary for metallic biomaterials to maintain satisfying mechanical properties and minimize the immune responses induced by corrosion products during service life. In particular, enhancing pitting corrosion resistance of the Ti-based glassy alloys is important to promote them to be as potential biomaterials.

In our previous study, it has been proved that the bio-corrosion resistance of the Ti–Zr–Cu–Fe–Sn–Si–Ag glassy alloys can be improved by minor alloying strongly passivating element Nb [19]. It is also noticed that Ta has been widely used in making surgical instruments and implants, since it resists attack by body fluids and is nonirritating [20]. Remarkable enhancement of corrosion resistance of some BMGs by the addition of Ta has been reported before [21–23]. It has been found that the Ta-incorporated Ti–Zr–Cu–Pd–Sn BMG exhibits better pitting corrosion resistance than that of Nb-incorporated Ti–Zr–Cu–Pd–Sn BMG in 0.144 mol·L^{-1} NaCl solution. However, the corrosion resistance of the Zr-based BMGs with Ta addition is slightly inferior than that of the Nb-bearing Zr-based BMGs [22]. Therefore, the influence of Ta and Nb content on corrosion resistance on BMGs is still in debate.

In this work, addition of Ta for replacing partial Cu of the Ti–Cu–Zr–Fe–Sn–Si–Ag BMG was conducted in order to further enhance the bio-corrosion resistance. The effects of Ta alloying on GFA, thermal properties, bio-corrosion behaviors in 0.9 wt% NaCl and Hank's solution as well as mechanical properties of the Ti-based BMGs were studied. The corresponding mechanisms of the glass formation and bio-corrosion behavior were also discussed.

2 Experimental

Alloy ingots with nominal compositions of $Ti_{47}Cu_{40-x}Zr_{7.5}Fe_{2.5}Sn_2Si_1Ta_x$ (x = 1–4; at%, the same below) were prepared by arc melting under a high-purity argon atmosphere. The mixture of Zr and Ta was melted initially to prepare a pre-alloy and then remelted with other pure elements. From the master alloys, glassy ribbons and rod samples were prepared by melt spinning and injection copper mold casting, respectively, under an argon atmosphere. Microstructure of the Ti-based alloys was characterized by X-ray diffractometer (XRD, Rigaku D/Max-2500) using Cu Kα radiation. Thermal properties of the samples were evaluated by a differential scanning calorimetry (DSC, RT-1600, Netzsch STA-449F3) at a heating rate of 0.33 K·s^{-1} under a flowing argon atmosphere.

The Ti-based glassy rod samples with diameter of 2 mm were adopted for evaluating the corrosion resistance, mechanical properties, Vicker microhardness as well as Young's modulus. Corrosion behaviors of the Ti-based glassy alloys in 0.9 wt% NaCl solution and Hank's solution were evaluated by electrochemical measurements. Commercial Ti–6Al–4V alloy, generally applied as orthopedic implants, was employed as the reference material. Before corrosion tests, the samples were mechanically polished up to 2000-grit silicon carbide paper and then were ultrasonic cleaned in acetone, absolute alcohol and deionized water sequentially. Finally, the samples were dried and exposed to air for about 24 h for good reproducibility. The three-electrode system consisting of a sample as the working electrode, a platinum counter electrode and a saturated calomel reference electrode (SCE, E_{SCE} = 0.242 V) was adopted to conduct electrochemical measurements. Anodic potentiodynamic polarization curves were measured from the potential of about 50 mV below the open-circuit potential (OCP) at a scan rate of 0.833 mV·s^{-1}, until the OCP achieves a stable value after immersion in artificial body fluids for 1800 s. Triplicate samples of each alloy were adopted to confirm the reproducibility.

The glassy rod samples with the length–diameter ratio of 2:1 were used to characterize the compressive mechanical properties of the Ti-based BMGs by a material testing machine at a constant strain rate of 2.0×10^{-4} s^{-1}. At least four tests of each alloy were conducted to confirm the reproducibility. Lateral and fracture surfaces of the deformed samples were observed by a scanning electron microscope (SEM, JEOL JSM-6010LA). Vicker microhardness of the glassy specimens was measured under a load of 2 N for 12 s using a Vicker microhardness tester (Future-tech FM800). The density of the Ti-based BMGs was measured by Archimedean principle using tetrabromoethane. Young's modulus (E) of the bulk glassy samples was calculated from transverse and longitudinal wave velocity measured by ultrasonic system (Olympus Panametrics-NDT 5703PR) [24].

3 Results and discussion

XRD patterns of the Ti-based alloy rod samples with diameter of 3 mm in Fig. 1 exhibit a main broad halo without crystalline peaks, indicating the formation of amorphous structure. Moreover, the critical diameter of the Ti-based BMGs maintains at 3 mm with Ta content increasing from 1 at% to 4 at%, suggesting that the minor addition of Ta has insignificant influence on GFA of the Ti-based BMGs. Figure 2a shows DSC curves of the ribbons and the rod samples with a diameter of 3 mm. The DSC

traces of all the Ti-based alloy samples were characterized by glass transition and subsequent supercooled liquid region followed by crystallization. Almost identical thermal behaviors for the ribbon and the rod sample of each alloy further confirm the glassy structure of the rod samples. Therefore, the critical diameter of the present Ti-based BMGs is 3 mm. The values of glass transition temperature (T_g), onset temperature of crystallization (T_x) and supercooled liquid region ($\Delta T_x = T_x - T_g$) as function of Ta content of the present Ti-based glassy alloys are summarized in Fig. 2b. It can be seen that ΔT_x gradually decreases from 54 to 45 K with Ta content increasing from 0 at% to 3 at% and 4 at%. The influence of Ta content on GFA of the present Ti-based BMGs could not be strictly illuminated by the change in the ΔT_x values, although ΔT_x and GFA of the Ti-based BMG decrease with the addition of 1 at% Ta. On the one hand, it is considered that large negative heats of mixing among the main constituent elements are beneficial for enhancing glass forming ability [12]. However, the mixing heat of Ta–Ti, Ta–Zr and Ta–Cu atomic pairs is 1, 3 and 2 kJ·mol^{-1} [25], respectively, which could lead to the instability of the supercooled liquid. The atomic pairs with positive mixing heat, exhibiting repulsive interaction, would be detrimental to the formation of dense random packed structures or atomic clusters, which would induce the nucleation and growth reactions of a crystalline phase, a lower viscosity and easier constituent element diffusion [26]. Hence, the addition of Ta is slightly detrimental to the GFA and thermal stability of the Ti–Cu–Zr–Fe–Sn–Si–Ag BMG. On the other hand, the mixing entropy increases with the addition of Ta in the Ti-based BMGs, which could not only confuse the phase nucleation and growth but also favor the glass formation [27]. Owing to the competition between the two glass formation mechanisms, the critical diameter of the Ti-based BMGs decreases from 7 to 3 mm with addition of 1 at% Ta and then shows insignificant change with Ta content further increasing up to 4 at%.

In order to understand the corrosion resistance of the present Ti-based BMGs in comparison with the commercial Ti–6Al–4V alloy in artificial body fluids and the effect of Ta on corrosion behavior, electrochemical measurements in 0.9 wt% NaCl solution and in Hank's solution

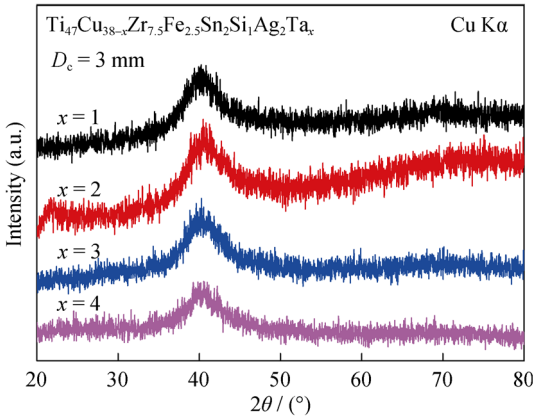

Fig. 1 XRD patterns of $Ti_{47}Cu_{38-x}Zr_{7.5}Fe_{2.5}Sn_2Si_1Ag_2Ta_x$ (x = 1–4) BMGs with their critical diameters prepared by injection copper mold casting

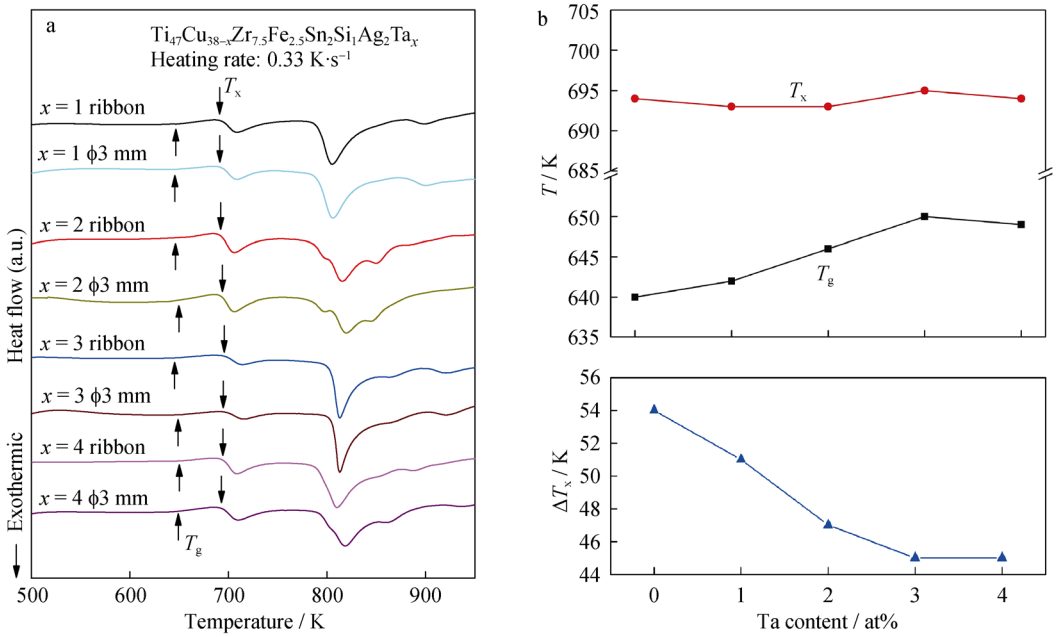

Fig. 2 **a** DSC curves of $Ti_{47}Cu_{38-x}Zr_{7.5}Fe_{2.5}Sn_2Si_1Ag_2Ta_x$ (x = 1–4) glassy ribbons and BMGs with their critical diameters; **b** changes in T_g, T_x and ΔT_x with Ta content of $Ti_{47}Cu_{38-x}Zr_{7.5}Fe_{2.5}Sn_2Si_1Ag_2Ta_x$ (x = 1–4) BMGs

containing Mg^{2+}, Ca^{2+} and glucose were carried out. Figure 4a shows the change in OCP with immersion time for the Ti-based BMGs in 0.9 wt% NaCl solution. For all the Ti-based BMGs, the OCP values are higher than that of the Ti–6Al–4V alloy and are stable as extending immersion time due to formation of stable passive oxide films. Additionally, the OCP value slightly increases from − 0.30 to − 0.25 V with addition of 2 at% Ta and then increases drastically up to about − 0.15 V when Ta content reaches above 3 at%. The enhanced OCP values suggest the improved stability of surface film on the Ti-based glassy alloys with Ta content increasing. Potentiodynamic polarization curves of the present Ti-based glassy alloys in 0.9 wt% NaCl solution are presented in Fig. 3b. All the Ti alloys spontaneously passivated with low passive current density around 1×10^{-6} to 1×10^{-5} A·cm^{-2}, although the Ti-based glassy alloys exhibit pitting corrosion at relative high potentials of above 0.75 V. With the Ta content of the Ti-based glassy alloys increasing from 1 at% to 4 at%, the passive current density gradually becomes lower, and the pitting corrosion potential increases from 0.75 to 1.25 V, implying that the addition of Ta is effective on improving corrosion resistance of the Ti-based glassy alloys in 0.9 wt% NaCl solution. As depicted in Fig. 4, the Ti-based glassy alloys exhibit similar corrosion behaviors in Hank's solution to those in 0.9 wt% NaCl solution. The OCP values of the Ti-based glassy alloys increase with Ta addition increasing and are higher than that of Ti–6Al–4V alloy. The polarization curves of the Ti-based glassy alloys indicate that they are spontaneously passivated, and their passive current densities are paralleled to that of Ti–6Al–4V alloy. Moreover, the pitting potentials of the glassy alloys become higher with Ta content increasing. The high total contents of Ti, Zr and Ta and the homogenous single-phase nature of the present Ti-based glassy alloy may lead to the formation of uniform passive film enriched in Ti, Zr and Ta on the alloy surface, which could be responsible for the high corrosion resistance [28–30]. Compared with the corrosion resistance of the reported Ti–Cu–Zr–Fe–Sn–Si–Ag–Nb BMG in Hank's solution, the Ti–Cu–Zr–Fe–Sn–Si–Ag–Ta BMG exhibits similar passive current density (1×10^{-6} to 1×10^{-5} A·cm^{-2}) and pitting potential [19]. Therefore, the addition of Ta or Nb is effective for enhancing corrosion resistance of the Ti–Cu–Zr–Fe–Sn–

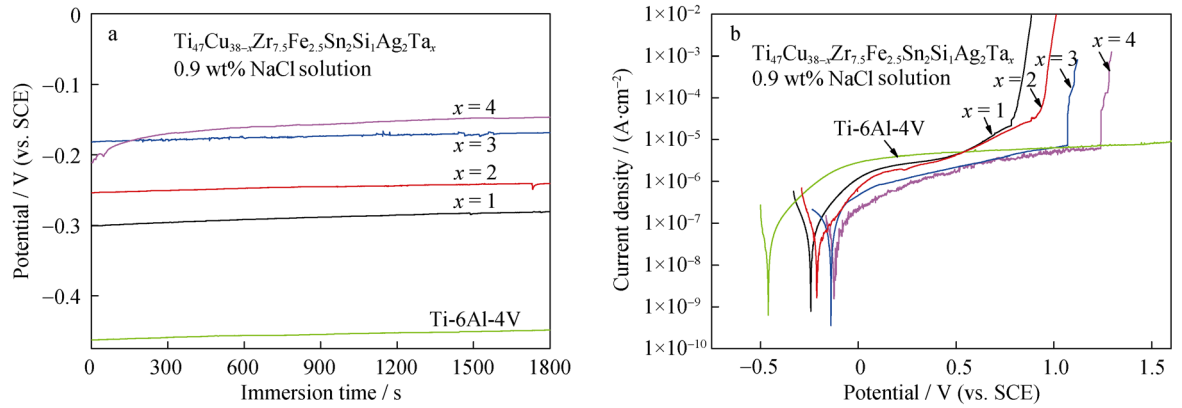

Fig. 3 **a** Changes in open-circuit potentials with immersion time and **b** potentiodynamic polarization curves of $Ti_{47}Cu_{38-x}Zr_{7.5}Fe_{2.5}Sn_2Si_1Ag_2Ta_x$ (x = 1–4) glassy alloys in 0.9 wt% NaCl solution

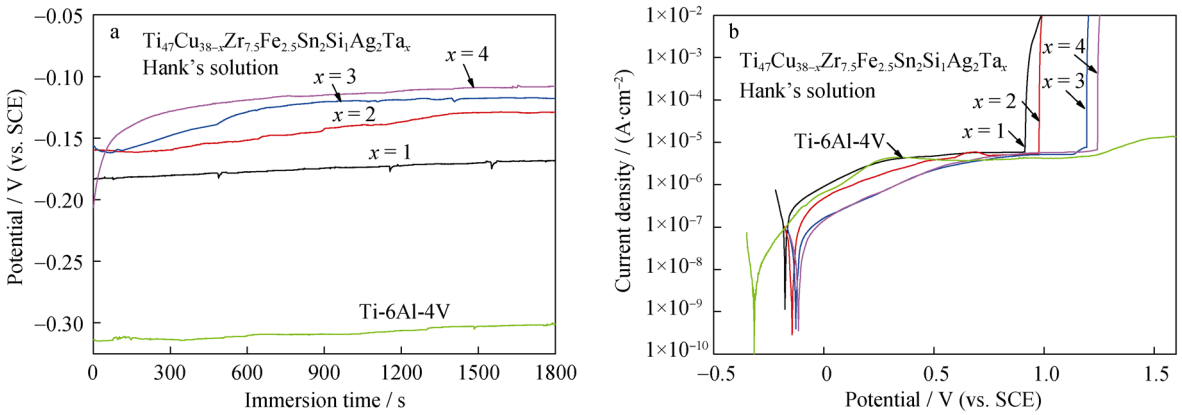

Fig. 4 **a** Changes in open-circuit potentials with immersion time and **b** potentiodynamic polarization curves of $Ti_{47}Cu_{38-x}Zr_{7.5}Fe_{2.5}Sn_2Si_1Ag_2Ta_x$ (x = 1–4) glassy alloys in Hank's solution

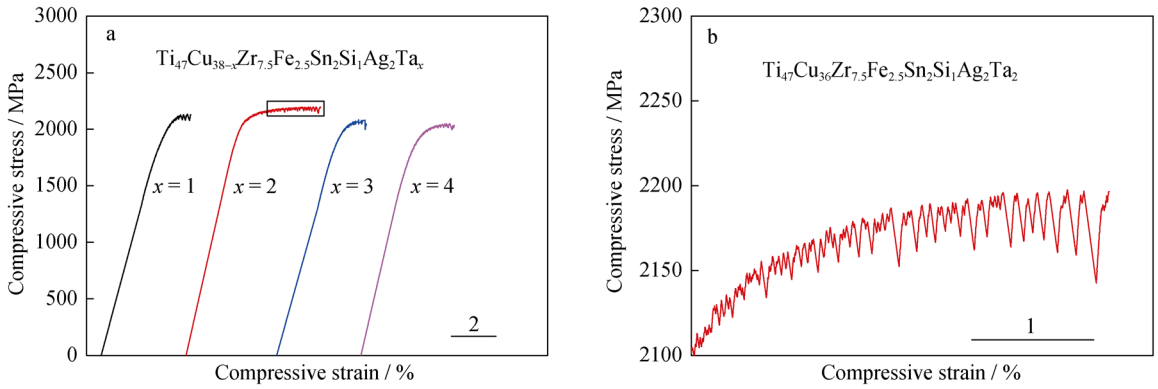

Fig. 5 **a** Compressive stress–strain curves of $Ti_{47}Cu_{38-x}Zr_{7.5}Fe_{2.5}Sn_2Si_1Ag_2Ta_x$ (x = 1–4) BMGs and **b** enlargement of serrations in framed region of stress–strain curve in **a**

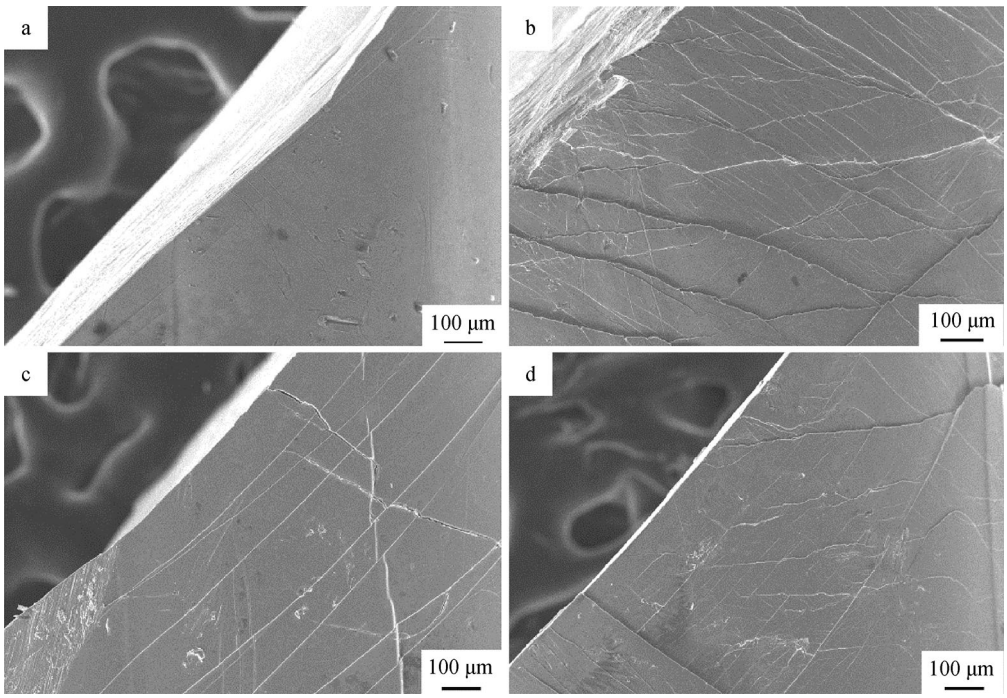

Fig. 6 SEM images of lateral surfaces of the $Ti_{47}Cu_{38-x}Zr_{7.5}Fe_{2.5}Sn_2Si_1Ag_2Ta_x$ BMGs after compressive deformation: **a** x = 1, **b** x = 2, **c** x = 3 and **d** x = 4

Si–Ag BMG though Ta and Nb alloying are slightly detrimental to the glass forming ability. The good corrosion resistance of the Ti-based BMGs is favorable for the biomedical application.

Figure 5a presents the compressive stress–strain curves of the Ti-based glassy rod samples with a diameter of 2 mm. It can be seen that the present Ti-based BMGs possess high fracture stress above 2000 MPa, a certain plastic strain as well as relative low Young's modulus around 100 GPa. It can also be seen that with Ta content increasing up to 2 at%, the fracture strength (σ_b) gradually increases to 2191 MPa and then decreases to 2014 MPa with the further increase in Ta content up to 4 at%. In the present glassy alloy system, the $Ti_{47}Cu_{36}Zr_{7.5}Fe_{2.5}Sn_2Si_1Ag_2Ta_2$ BMG exhibits the optimal

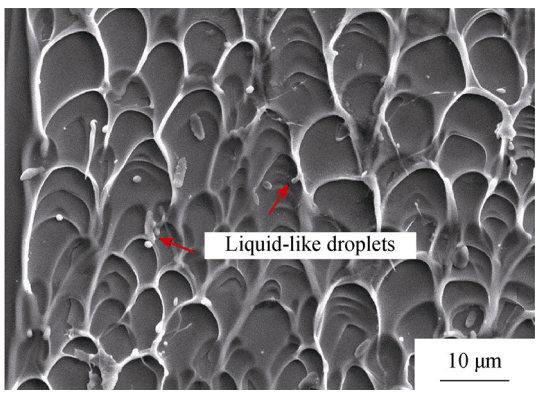

Fig. 7 SEM image of $Ti_{47}Cu_{36}Zr_{7.5}Fe_{2.5}Sn_2Si_1Ag_2Ta_2$ BMG after compressive deformation

Table 1 Densities, mechanical properties and elastic properties of $Ti_{47}Cu_{38-x}Zr_{7.5}Fe_{2.5}Sn_2Si_1Ag_2Ta_x$ (x = 0–4) BMGs

Alloy	σ_y/MPa	σ_f/MPa	ε_p/%	Hardness (HV)	Density/(g·cm^{-3})	E/GPa
x = 0 [3]	2028 ± 32	2081 ± 18	2.5	588 ± 6	6.238	100.4 ± 0.2
x = 1	1952 ± 36	2126 ± 57	1.1 ± 0.2	592 ± 5	6.390	100.5 ± 0.4
x = 2	2022 ± 43	2191 ± 45	3.4 ± 0.4	595 ± 6	6.485	100.2 ± 0.3
x = 3	1969 ± 48	2080 ± 43	1.0 ± 0.2	588 ± 4	6.612	98.6 ± 0.5
x = 4	1878 ± 45	2041 ± 50	1.8 ± 0.2	582 ± 4	6.642	98.4 ± 0.7

integrated mechanical properties, such as the highest fracture strength of about 2191 MPa and largest plastic strain of about 3.4%. Figure 5b shows the partial enlargement of the stress–strain curve for the $Ti_{47}Cu_{36}Zr_{7.5}Fe_{2.5}Sn_2Si_1Ag_2Ta_2$ BMG. A large serration event following a succession of serration events with smaller amplitude can be observed, suggesting the generation of secondary shear bands followed by the emission of a primary shear band [31–33]. SEM images of the lateral and fracture surface of deformed samples are shown in Fig. 6. As depicted in Fig. 6a–d, the fracture surface inclines by about 40° to the direction of the applied compressive load. Shear bands with high density, generating during plastic deformation, can be observed on the lateral surfaces. The larger plasticity of the Ti-based BMGs corresponds to the more shear bands observed on their lateral surfaces of the failed samples. The largest number of shear bands, including the primary shear bands parallel to the fracture plane and the secondary shear bands with irregular orientations, can be observed on the lateral surface of the $Ti_{47}Cu_{36}Zr_{7.5}Fe_{2.5}Sn_2Si_1Ag_2Ta_2$ sample. The fracture surface exhibits well-developed vein pattern, which is a typical feature for ductile BMGs (Fig. 7). Liquid-like droplets are also seen on the fracture surface, implying local softening and/or melting during compression. By ultrasound velocity measurement, Young's modulus of the Ti-based BMGs is determined to be 98.4–100.4 GPa. The densities, mechanical properties and Young's modulus of the Ti-based BMGs as well as Ti–6Al–4V alloy are summarized in Table 1. The microhardness of the Ti-based BMGs in the range of HV 582–HV 595 is much higher than that of the Ti–6Al–4V alloy, implying better wear resistance according to Archard's wear equation [4, 34]. Young's modulus of the Ti-based BMGs (98.4–100.4 GPa) is lower than that of Ti–6Al–4V alloy (∼ 110 GPa), which is beneficial for alleviating stress shielding effect as potential implant biomaterials [35].

4 Conclusion

$Ti_{47}Cu_{38-x}Zr_{7.5}Fe_{2.5}Sn_2Si_1Ag_2Ta_x$ (x = 1–4) BMGs with a critical diameter of 3 mm can be prepared by copper mold casting. The supercooled liquid region of the Ti-based glassy alloys gradually decreases from 51 to 45 K with the increase of Ta content. The present Ti-based BMGs exhibit higher open-circuit potential, lower passive current density and improved pitting corrosion resistance in 0.9 wt% NaCl and Hank's solutions by increasing Ta content. The Ti-based BMG with 2 at% Ta content presents the optimal integration of mechanical properties, including compressive fracture strength of ∼ 2000 MPa, relative low Young's modulus of ∼ 98 GPa and plastic strain of ∼ 3.4% as well as high hardness of ∼ HV 599. The good combination of relative high GFA, good bio-corrosion resistance and mechanical properties of the Ti-based BMGs suggests their potential as biomaterials.

Acknowledgements This work was financially supported by the National Natural Science Foundation of China (Nos. 51671008 and 51701008), the Aeronautical Science Foundation of China (No. 2013ZE51060) and China Postdoctoral Science Foundation (No. 2017M620575).

References

[1] Schroers J, Kumar G, Hodges TM, Chan S, Kyriakides TR. Bulk metallic glasses for biomedical applications. JOM. 2009;61(9):21.
[2] Xie GQ, Qin FX, Zhu SL. Recent progress in Ti-based metallic glasses for application as biomaterials. Mater Trans. 2013;54(8):1314.
[3] Pang SJ, Liu Y, Li HF, Sun LL, Li Y, Zhang T. New Ti-based Ti–Cu–Zr–Fe–Sn–Si–Ag bulk metallic glass for biomedical applications. J Alloys Compd. 2015;625:323.
[4] Liu Y, Wang G, Li HF, Pang SJ, Chen KW, Zhang T. Ti–Cu–Zr–Fe–Sn–Si–Sc bulk metallic glasses with good mechanical properties for biomedical applications. J Alloys Compd. 2016;679:341.
[5] Liu Y, Pang SJ, Li HF, Hu Q, Chen B, Zhang T. Formation and properties of Ti-based Ti–Zr–Cu–Fe–Sn–Si bulk metallic glasses with different (Ti + Zr)/Cu ratios for biomedical application. Intermetallics. 2016;72:36.
[6] Wang YB, Li HF, Cheng Y, Zheng YF, Ruan LQ. In vitro and in vivo studies on Ti-based bulk metallic glass as potential dental implant material. Mater Sci Eng C. 2013;33(6):3489.
[7] Li HF, Zheng YF. Recent advances in bulk metallic glasses for biomedical applications. Acta Biomater. 2016;36:1.
[8] Oak JJ, Inoue A. Attempt to develop Ti-based amorphous alloys for biomaterials. Mater Sci Eng A. 2007;449(13):220.
[9] Calin M, Gebert A, Ghinea AC, Gostin PF, Abdi S, Mickel C, Eckert J. Designing biocompatible Ti-based metallic glasses for implant applications. Mater Sci Eng A. 2013;33(2):875.

[10] Oak JJ, Louzguine-Luzgin DV, Inoue A. Fabrication of Ni-free Ti-based bulk metallic glassy alloy having potential for application as biomaterial, and investigation of its mechanical properties, corrosion, and crystallization behavior. J Mater Res. 2007;22(5):1346.
[11] Suryanarayana C, Inoue A. Bulk Metallic Glasses. Boca Raton: CRC Press; 2011. 1.
[12] Inoue A. Stabilization of metallic supercooled liquid and bulk amorphous alloys. Acta Mater. 2000;48(1):279.
[13] Greer AL. Confusion by design. Nature. 1993;366(6453):303.
[14] Zhang T, Li R, Pang SJ. Effect of similar elements on improving glass-forming ability of La–Ce-based alloys. J Alloys Compd. 2009;483(1):60.
[15] Kamachi Mudali U, Sridar TM, Raj B. Corrosion of bio implants. Sadhana. 2003;28(3–4):601.
[16] Kamachi Mudai U, Baunack S, Eckert J, Schultz L, Gebert A. Pitting corrosion of bulk glass-forming zirconium-based alloys. J Alloys Compd. 2004;377(1):290.
[17] Hanawa T. Evaluation techniques of metallic biomaterials in vitro. Sci Technol Adv Mater. 2002;3(4):289.
[18] Jin K, Loffler JF. Bulk metallic glass formation in Zr–Cu–Fe–Al alloys. Appl Phys Lett. 2005;86(24):3.
[19] Yan HM, Liu Y, Pang SJ. Glass formation and properties of Ti-based bulk metallic glasses as potential biomaterials with Nb addition. Rare Met. 2015. https://doi.org/10.1007/s12598-015-0664-5.
[20] Buckman RW. New applications for tantalum and tantalum alloys. JOM. 2000;52(3):40.
[21] Qin FX, Wang XM, Kawashima A, Zhu SL, Kimura H, Inoue A. Corrosion behavior of Ti-based metallic glasses. Mater Trans. 2006;47(8):1934.
[22] Li YH, Zhang W, Dong C, Yamaura S, Makino A. Glass-forming ability, corrosion resistance and mechanical properties of $Zr_{60-x}Al_{15}Ni_{25}TM_x$ (TM = Nb and Ta) bulk metallic glasses. Mater Trans. 2013;54(8):1368.
[23] Qin FX, Zhou Y, Ji C, Dan ZH, Xie GQ, Yang S. Enhanced mechanical properties, corrosion behavior and bioactivity of Ti-based bulk metallic glasses with minor addition elements. Acta Metall Sin. 2016;29(11):1011.
[24] Wang WH. The elastic properties, elastic models and elastic perspectives of metallic glasses. Prog Mater Sci. 2011;57(3):487.
[25] Takeuchi A, Inoue A. Classification of bulk metallic glasses by atomic size difference, heat of mixing and period of constituent elements and its application to characterization of the main alloying element. Mater Trans. 2005;46(12):2817.
[26] Inoue A, Shibata T, Zhang T. Effect of additional elements on glass transition behavior and glass formation tendency of Zr–Al–Cu–Ni alloys. Mater Trans JIM. 1995;36(12):1420.
[27] Guo S, Liu CT. Phase stability in high entropy alloys: formation of solid-solution phase or amorphous phase. Prog Nat Sci Mater. 2011;21(6):433.
[28] Vasilescu C, Drob SI, Calderon Moreno JM, Osiceanu P, Popa M, Vasilescu Marcu M, Drob P. Long-term corrosion resistance of new Ti–Ta–Zr alloy in simulated physiological fluids by electrochemical and surface analysis methods. Corros Sci. 2015;93:310.
[29] Qin CL, Asami K, Kimura H, Zhang W, Inoue A. Electrochemical and XPS studies of Ni-based metallic glasses in boiling nitric acid solutions. Electrochim Acta. 2009;54(5):1612.
[30] Hashimoto K, Habazaki H, Akiyama E, Yoshioka H, Kim JH, Park PY, Kawashima A, Asami K. Recent progress in corrosion-resistant metastable alloys. Sci Rep RITU. 1996;A42:99.
[31] Song SX, Bei H, Wadsworth J, Nieh TG. Flow serration in a Zr-based bulk metallic galss in compression at low strain rates. Intermetallics. 2008;16:813.
[32] Wright WJ, Saha R, Nix WD. Deformation of The $Zr_{40}Ti_{14}Ni_{10}Cu_{12}Be_{24}$ bulk metallic glass. Mater Trans. 2001;42(4):642.
[33] Zhang Y, Liu JP, Chen SY, Xie X, Peter KK, Dahmen KA, Qiao JW, Wang YL. Serration and noise behaviors in materials. Prog Mater Sci. 2017;90:358.
[34] Archard JF. Contact and rubbing of flat surface. J Appl Phys. 1953;24(8):981.
[35] Chen QZ, Thouas AG. Metallic implant biomaterials. Mater Sci Eng R. 2015;87:1.